Eur. Phys. J. A **16**, 193–197 (2003)
DOI 10.1140/epja/i2002-10087-7

THE EUROPEAN PHYSICAL JOURNAL A

Kinematical separation of α-n final-state interaction at 50 MeV incident energy

S. Dey (Mandal)[1,a], S.S. Dasgupta[1], C.C. Dey[2], and P. Bhattacharya[2]

[1] Department of Physics, The University of Burdwan, Burdwan - 713104, India
[2] Saha Institute of Nuclear Physics, 1/AF, Bidhannagar, Kolkata - 700064, India

Received: 17 June 2002 / Revised version: 27 September 2002 /
Published online: 4 February 2003 –
Communicated by M. Garçon

Abstract. A kinematically complete experiment has been performed to study the α-n final-state interaction (FSI) in the $\alpha + \mathrm{d} \rightarrow \alpha + \mathrm{p} + \mathrm{n}$ break-up reaction at 50 MeV incident energy for the alpha-particles. For this, we have chosen four pairs of correlation angles for the outgoing alpha and protons. These are ($\theta_\alpha = 18^\circ$, $\theta_\mathrm{p} = 42^\circ$), ($\theta_\alpha = 20^\circ$, $\theta_\mathrm{p} = 45^\circ$), ($\theta_\alpha = 22^\circ$, $\theta_\mathrm{p} = 42^\circ$) and ($\theta_\alpha = 22^\circ$, $\theta_\mathrm{p} = 47^\circ$), selected kinematically where the allowed phase spaces are in favor of the α-n final-state interaction. Our experimental data show strong α-n FSI in all the selected configurations. Also, the FSI is found to be stronger at the lower alpha-particle energy when two FSI peaks appear in the same configuration.

PACS. 25.55.-e ^{3}H-, ^{3}He-, and ^{4}He-induced reactions – 25.10.+s Nuclear reactions involving few-nucleon systems

1 Introduction

The α-induced deuteron break-up experiments help us to understand the nature of nuclear force, particularly, to find whether there is any effect of three-body interaction in the nuclear force. This is because, below the α break-up threshold, there are three particles in the final state, viz, the α, proton and neutron and both two-body and three-body interactions in the final state are possible. A great deal of effort has been given to study the FSI in α-induced deuteron break-up, both theoretically and experimentally [1–16]. Below the alpha break-up threshold, the report of FSI studies in the α-induced deuteron break-up is available at several incident energies for the alpha-particles (E_α(inc)). For incident energies between 9.735 and 11.30 MeV (close to the deuteron break-up threshold) and using a gas target, Dasgupta *et al.* [2,3] studied FSI in the α-induced deuteron break-up at a fixed correlation angle for the outgoing proton and alpha-particles ($\theta_\alpha = 15^\circ$, $\theta_\mathrm{p} = 30^\circ$). However, they observed overlapping of different FSIs (α-p and α-n) and α-p quasi-free scattering (QFS). The overlapping of different phase spaces was due to low kinetic energies of the outgoing particles. At E_α(inc) = 15 MeV, Koersner *et al.* [4] studied the α-d break-up reaction for eleven correlation angles. They analysed the data in semi-phenomenological impulse approximation. The discrepancies between the theoretical fit and the experimental data were explained by the prediction of triton transfer reaction. But, Y. Koike [5] explained the discrepancies as due to a large interference between α-n and α-p FSI. Glantz *et al.* [6] also observed interference between α-n and α-p FSI in the same configuration in a kinematically complete experiment of ^{2}H(α, αp)n reaction at E_α(inc) = 13, 15 and 18 MeV. The same ^{2}H(α, αp)n reaction was studied by Rausch *et al.* [7] at incident energies E_α(inc) = 21.9 and 23.7 MeV also in a kinematically

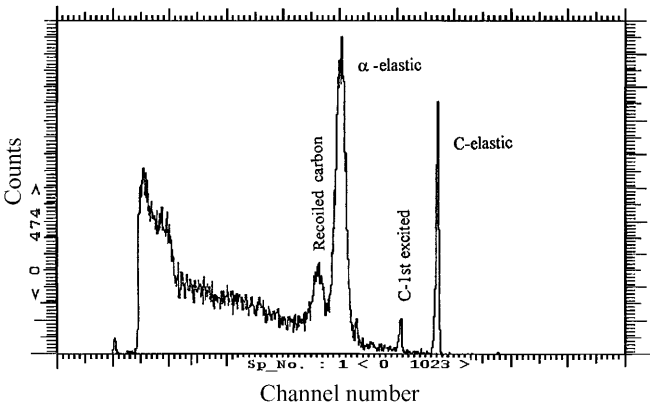

Fig. 1. A coincidence spectrum for break-up events in the alpha detector at $\theta_\alpha = 22^\circ$. Continuous distribution of energies below the recoiled carbon peak are due to the break-up events.

[a] e-mail: dey_s2001@yahoo.com; *Present address*: 445 Waupelani Drive, Apt. F3, State College, PA 16801, USA.

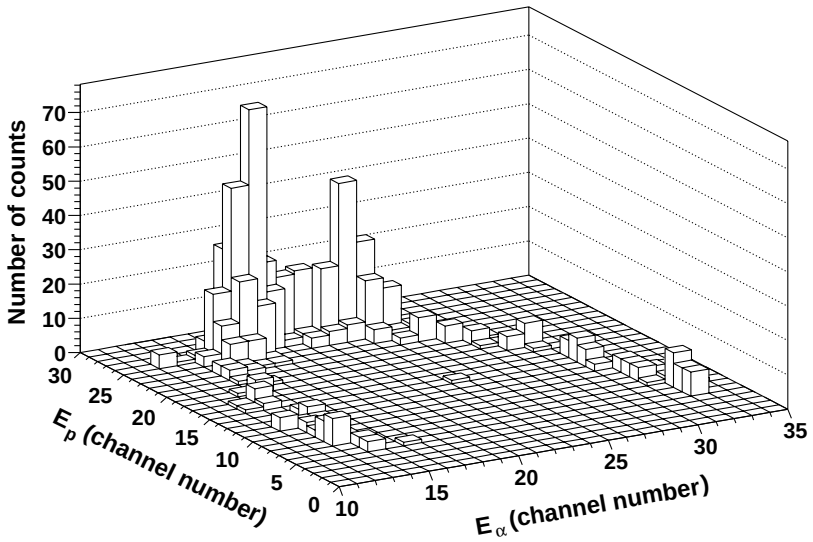

Fig. 2. A 2D E_α-E_p plot at the correlation angles ($\theta_\alpha = 20°$, $\theta_\mathrm{p} = 45°$). The number of counts corresponding to each point in the plot is shown.

complete experiment, suitable for observing α-p QFS and n-p FSI. Their observation, however, showed α-p FSI and QFS along with the n-p FSI. Bruno *et al.* [8] studied the deuteron break-up reaction at incident alpha-particle energies between 9.847 and 13.991 MeV for 21 correlation angles. The data were compared with the predictions based on Faddeev equations. They observed interference between α-n and α-p FSI. The interference was mainly due to low kinetic energies which produced small kinematical loci. Warner and Bercaw [9] studied the above reaction at higher incident energy (E_α(inc) = 42 MeV) and at several correlation angles to observe the α-n FSI. Here, in the same correlation angle, they observed prominent peaks due to ^{5}He and ^{5}Li FSI and broad spectator peaks (QFS) overlapping with each other. At two pairs of correlation angles ($\theta_\alpha = 19.8°$, $\theta_\mathrm{p} = 40°$) and ($\theta_\alpha = 19.8°$, $\theta_\mathrm{p} = 50°$), only the α-n FSI was found to be strong. Thus, in most of the earlier studies, at incident energies between 9.735 and 42 MeV, interferences between different two-body final-state interactions (α-n, α-p and n-p) and also α-p quasi-free scattering were found. Y. Koike [5] analysed the above experimental data at energies 15–42 MeV by the Amado-Lovless equations. Koike pointed out that one reason for discrepancies between theory and experiment was due to a large interference between different FSIs, since, α-n and α-p FSI peaks were kinematically very close to each other.

Recently De *et al.* [16], using 45 MeV energy for the incident α-particle, reported a three-body effects in the nuclear force from their measured cross-section at one pair of correlation angles ($\theta_\alpha = 20°$, $\theta_\mathrm{p} = 54°$). This was inferred from the enhancement they observed in the collinearity region ($E_\mathrm{n}^\mathrm{CM} = 0$) of the measured cross-section. The present experiment has been performed to separate the α-n FSI from other two-body interactions. For this, we have judiciously selected the incident alpha-particle energy (50 MeV) and the pair of correlation angles from kinematical considerations [17], where only the α-n FSI were expected in the allowed phase space. The correlation angles for the alpha and protons chosen in the present experiment are ($\theta_\alpha = 18°$, $\theta_\mathrm{p} = 42°$), ($\theta_\alpha = 20°$, $\theta_\mathrm{p} = 45°$), ($\theta_\alpha = 22°$, $\theta_\mathrm{p} = 42°$) and ($\theta_\alpha = 22°$, $\theta_\mathrm{p} = 47°$).

2 Experimental procedure

A beam of alpha-particles of 50 MeV energy from the cyclotron of Variable Energy Cyclotron Centre (VECC), Kolkata, India was used for the experiment. A solid polyethelyne target $(CD_2)_\mathrm{n}$ of 98% purity (thickness $\sim$ 720 μgm/cm^2) was used in the experiment. To avoid burning of the target, the beam current was kept less than 2 nA. For detecting the alpha and protons, the detectors used were ORTEC surface barrier. For the alpha detector, the thickness was 1 mm and for the proton, it was a 5 mm (E-ΔE) telescope. The thickness of the ΔE detector was 300 μm. Tantalum collimators were used for all the detectors. A detector of 500 μm thickness was used as monitor. The proton and alpha detectors were mounted on two different arms in a 90 cm scattering chamber of VECC. The two arms were placed on two opposite sides of the beam and in the same plane with the beam. The break-up data were taken in list mode and were analysed later off-line. For energy calibration of the detectors, α-d elastic coincidence data were taken in both the alpha and proton detectors at several angles. A coincidence spectrum for the break-up events in the alpha detector is shown in fig. 1. The coincidence spectra were generated by setting the peak in the time-to-amplitude conversion (TAC) spectrum between the alpha and proton detectors as gate.

From the coincidence energy spectra in the alpha (E_α) and proton (E_p) detectors, we generated two-dimensional (2D) E_α-E_p plots in 64×64 channels. A typical 2D spectrum is shown in fig. 2. The corresponding energy calibration for 2D spectra was done from the coincidence elastic data in the two detectors. The data points are found to be on the kinematical locus. The spreading of data is due to the finite angular openings of the detectors ($\pm 1°$). The

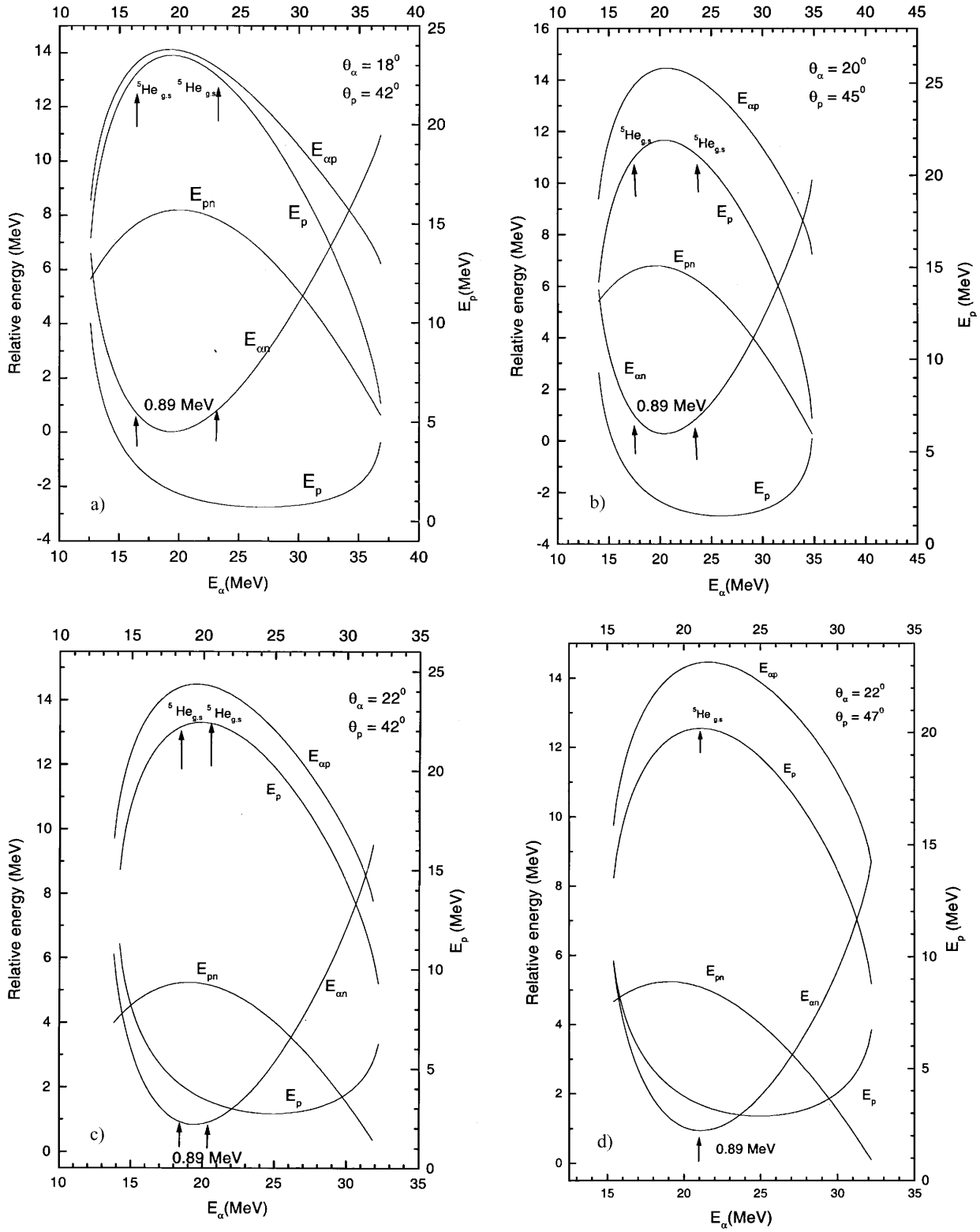

Fig. 3. Relative energy curves superimposed on kinematical energy loci for 50 MeV incident energy at the correlation angles $\theta_\alpha = 18°$, $\theta_\mathrm{p} = 42°$ (a), $\theta_\alpha = 20°$, $\theta_\mathrm{p} = 45°$ (b), $\theta_\alpha = 22°$, $\theta_\mathrm{p} = 42°$ (c) and $\theta_\alpha = 22°$, $\theta_\mathrm{p} = 47°$ (d).

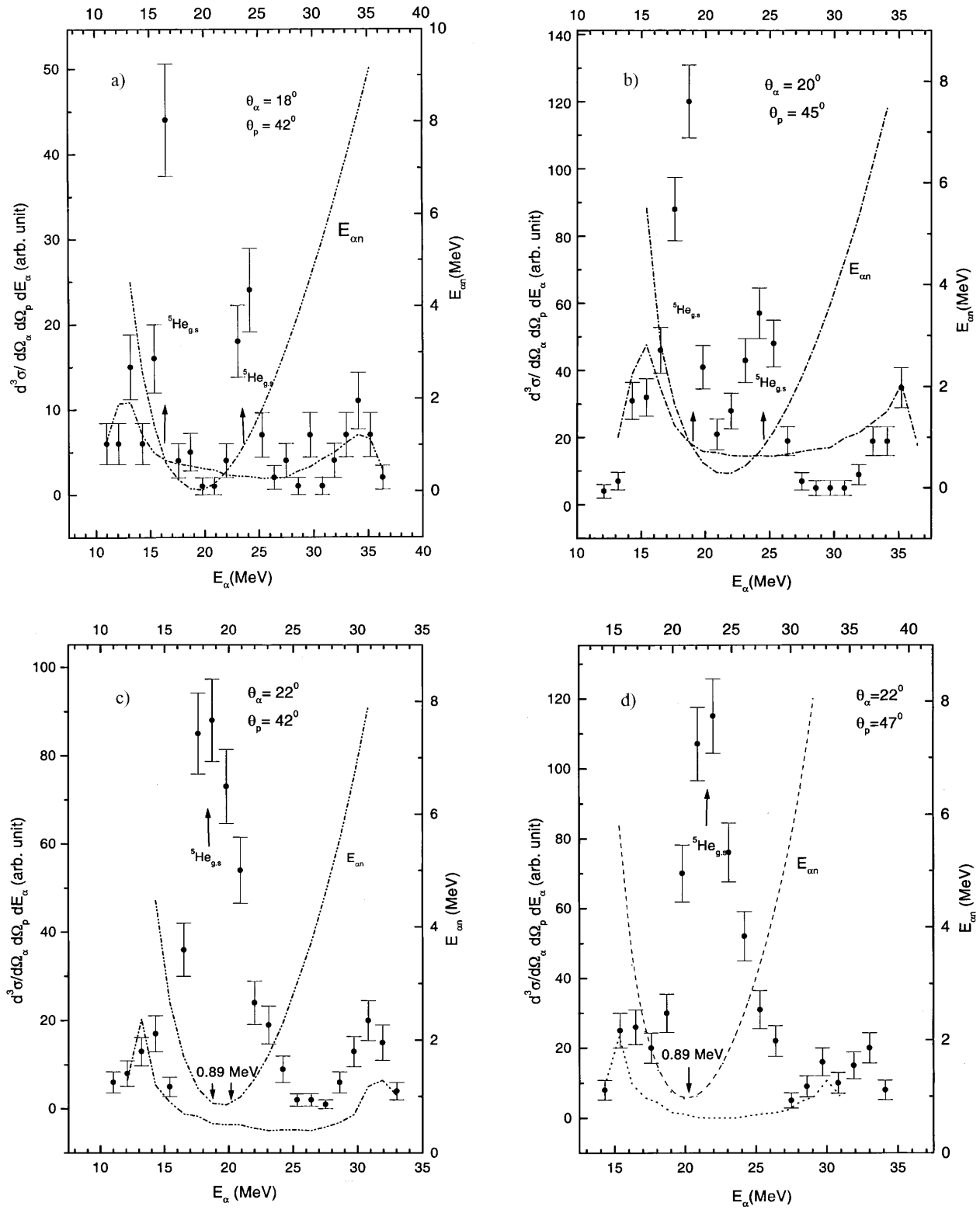

Fig. 4. Differential cross-sections *vs.* E_α at the correlation angles $\theta_\alpha = 18°$, $\theta_\mathrm{p} = 42°$ (a), $\theta_\alpha = 20°$, $\theta_\mathrm{p} = 45°$ (b), $\theta_\alpha = 22°$, $\theta_\mathrm{p} = 42°$ (c) and $\theta_\alpha = 22°$, $\theta_\mathrm{p} = 47°$ (d). The curves $E_{\alpha\mathrm{n}}$ are the α-n relative energies *vs.* E_α. Arrows indicate the positions of $^5\mathrm{He}_{\mathrm{g.s.}}$ The phase space curves are also shown in the figures.

number of events have been projected on the α-particle energy axis for each 2D plot and the data have been analysed from a kinematical point of view as follows.

3 Analysis and discussions

The kinematical plots of relative energies of the three final particles $E_{\alpha n}$, $E_{\alpha p}$ and E_{pn} [9] are shown in fig. 3 along with the kinematical energy locus (E_α-E_p). The formation of ^{5}He ground state is expected in the intermediate state due to α-n FSI when $E_{\alpha n} = 0.89$ MeV (excitation energy of ^{5}He ground state). The α-p and n-p FSIs are expected if $E_{\alpha p} = 1.965$ MeV and $E_{np} = 0$ MeV. Detailed calculations have been done in ref. [18]. From fig. 3(a)-(d), it is clear that only the α-n FSI is allowed kinematically. The α-p and n-p FSIs are not expected at our correlation angles. The QFS is also not allowed kinematically at these correlation angles.

The triple correlation cross-sections along with phase spaces and alpha-neutron relative energies ($E_{\alpha n}$) for different correlation angles are shown in fig. 4. For the correlation angles ($\theta_\alpha = 18°$, $\theta_p = 42°$), minima of $E_{\alpha n}$ is less than 0.9 MeV. So, there are two values of E_α, at ≈ 16 MeV and ≈ 23 MeV, corresponding to $E_{\alpha n} \approx 0.9$ MeV, and we expect two α-n FSI peaks at ≈ 7 MeV apart from each other on the upper half of the locus. The second and third peaks from left (fig. 4a) are very close to the predicted positions of α-n FSI peaks, at $E_\alpha \approx 16$ and 23 MeV, respectively. Therefore, we can identify these two peaks as due to α-n FSI as other interactions are not allowed kinematically. The first and last peaks are due to phase space. This arises due to projection of data on the E_α-axis. The data in the 2D plot are scattered in a band around the kinematic locus (fig. 2) due to the finite angular openings of the detectors ($\pm 1°$). The phase space has been obtained by the projection of the contour area on the E_α-axis.

In case of ($\theta_\alpha = 20°$, $\theta_p = 45°$), two α-n FSI peaks are expected kinematically (fig. 3b). The experimental E_α-E_p plot showed enhancements at two distinct positions. The second and third peaks (fig. 4b), arising from this enhancements, tally with the expected α-n FSI peaks. Here, the FSI peaks are closer (≈ 6 MeV) than that at the correlation angles ($\theta_\alpha = 18°$, $\theta_p = 42°$) as expected from kinematics. The two extreme peaks are due to phase space.

At the correlation angles ($\theta_\alpha = 22°$, $\theta_p = 42°$), two α-n FSI peaks are expected kinematically (fig. 3c) which are very close to each other (separation ≈ 1 MeV). Our experimental data (fig. 4c) show one broader peak in the α-n FSI region due to overlapping of these two α-n FSI peaks. Other peaks are due to phase space.

Finally, we consider the correlation angles ($\theta_\alpha = 22°$, $\theta_p = 47°$). The 2D E_α-E_p plot at this pair of correlation angles showed enhancement at a single position. Figure 4d, corresponding to this pair, shows also a single α-n FSI peak at $E_\alpha \approx 21$ MeV. At this pair of correlation angles only one α-n FSI peak at $E_\alpha \approx 21$ MeV is allowed also kinematically (fig. 3d) and is thus tallying with our experimental data. Thus, for all four pairs of correlation angles we have selected, the α-n FSI are found to be present strongly and there is no interference of other final-state interactions.

The other point we observe from the present experiment is that when there are two α-n FSI peaks at the same correlation angles (fig. 4a and b), we find that the cross-section is higher at lower α-particle energy and it is lower at higher energy. Since, here, there is no interference from other interactions, we can conclude that α-n FSI is stronger at lower α-particle energy. This can be explained as follows. At lower α-particle energy, the probability of forming the intermediate state is expected to be larger since there is more time to form the state resulting a higher cross-section. Warner and Bercaw [9] also found the similar thing at the correlation angles ($\theta_\alpha = 19.8°$, $\theta_p = 40°$) and ($\theta_\alpha = 19.8°$, $\theta_p = 50°$) where there were no interferences.

The triple correlation cross-section data of De *et al.* [16] at 45 MeV incident energy for the correlation angles ($\theta_\alpha = 20°$, $\theta_p = 54°$) showed an enhancement in the collinearity region ($E_n^{CM} = 0$) which they described as a possible indication of three-body effects of nuclear force. However, such enhancements were not observed from our measurements. In our case, the collinearity region lies at $E_\alpha \approx 20.4$ MeV for the correlation angles ($\theta_\alpha = 20°$, $\theta_p = 45°$) and is in between the two FSI peaks. Here, the two FSI peaks are clearly separated (fig. 4b) and there is no enhancement in the collinearity region.

References

1. R.J. Slobodrian, Rep. Prog. Phys. **34**, 175 (1971) and references therein.
2. S.S. Dasgupta, R.J. Slobodrian, R. Ray, C. Rioux, F. Lahlou, Phys. Rev. C **22**, 1815 (1980).
3. S.S. Dasgupta, R. Ray, C. Rioux, F. Lahlou, R.J. Slobodrian, Phys. Lett. B **91**, 32 (1980).
4. I. Koersner, L. Glantz, A. Johansson, B. Sandquist, H. nakamura, H. Noya, Nucl. Phys. A **286**, 431 (1977).
5. Y. Koike, Nucl. Phys. A **301**, 411 (1978).
6. L. Glantz, I Koersner, G. Jansen, A. Johansson, B. Sundquist, Nucl. Phys. A **390**, 365 (1982).
7. T. Rausch, H. Zell, D. Wallenwein, W. von Witsch, Nucl. Phys. A **222**, 429 (1974).
8. M. Bruno, F. Cannata, M. D' Agostino, M.L. Fiandri, M. Frisoni, G. Vannini, M. Lombardi, Nucl. Phys. A **386**, 269 (1982).
9. R.E. Warner, R.W. Bercaw, Nucl. Phys. A **109**, 205 (1968).
10. K. Sagara, T. Motobayashi, N Takahashi, Y. Hashimoto, M. Hara, Y. Nogami, H. Noya, H. Nakamura, Nucl. Phys. A **273**, 493 (1976).
11. T. Tanebe, J. Phys. Soc. Jpn. **25**, 21 (1968).
12. H. Nakamura, Nucl. Phys. A **208**, 207 (1973).
13. Y. Koike, Prog. Theor. Phys. **59**, 87 (1978).
14. N.O. Gaiser, S.E. Darden, R.C. Luhn, H. Paetz gen. Schieck, S. Sen, Phys. Rev. C **38**, 1119 (1988).
15. A. De, S.S. Dasgupta, D. Sen, Il Nuovo Cimento A **106**, 611 (1993).
16. A. De, S.S. Dasgupta, D. Sen, S.N. Chintalapudi, Few-Body Syst. **19**, 195 (1995).
17. G.G. Ohlsen, Nucl. Instrum. Methods **37**, 240 (1965).
18. S. Mandal (Dey), PhD Thesis (2001) unpublished.